의학석사 학위논문

두 가지 유형의 조직 공학 스캐폴드를 사용한 이상적인 식도 재건에 대한 쥐 모델 실험 연구

An experimental study for the ideal esophageal reconstruction with two different types of tissue-engineered scaffolds in a rat model

2020 년 2 월

서울대학교 대학원

의학과 이비인후과학 전공

박 하나로

두 가지 유형의 조직 공학 스캐폴드를 사용한 이상적인 식도 재건에 대한 쥐 모델 실험 연구

지도교수 정 은 재

이 논문을 의학 석사학위논문으로 제출함

2019 년 10 월

서울대학교 대학원

의학과 이비인후과학 전공

박 하나로

박하나로의 의학석사 학위논문을 인준함

2020 년 1 월

위 원 장 안 순 현 (인)

부위원장 정 은 재 (인)

위 원 권 성 근 (인)

An experimental study for the ideal esophageal reconstruction with two different types of tissue-engineered scaffolds in a rat model

by
Hanaro Park

A Thesis submitted to the Department of Otorhinolaryngology in partial fulfillment of the requirements for the Degree of Master of Science in Otorhinolaryngology at Seoul National University College of Medicine

January 2020

Approved by Thesis Committee:

Professor Ahn Soon-Hyun Chairman

Professor Chung Eun-Jae Vice chairman

Professor Kwon Seong Keun

ABSTRACT

An experimental study for the ideal esophageal reconstruction with two different types of tissue-engineered scaffolds in a rat model

Hanaro Park

Department of Otorhinolaryngology

The Graduate School of Medicine

Seoul National University

Introduction: Esophagus reconstruction, which is sometimes required to treat certain diseases of the esophagus, is associated with several morbidity and mortality. However, tissue engineering method offers promising alternative strategies. In this study, we evaluate the outcomes of esophageal reconstructions on rat model for partial esophageal defects using scaffolds made from two different types, respectively and to analyze the characteristics of each scaffolds.

Methods: Partial esophageal defects (1.5 × 2 mm, about one thirds

of circumference) was induced in rat models. The animals were divided into four groups depending on the scaffolds implanted in them: 3-dimensional printing (3DP) polycaprolactone (PCL) scaffolds, human adipose derived mesenchymal stem cells (hMSCs)-seeded 3DP scaffolds, electrospun nanofiber (EN) polyurethane (PU) scaffolds and hMSCs-seeded EN scaffolds. One- and four-weeks post-operation, the implanted sites were examined, and physical condition, body weight, and blood parameters were evaluated radiologically and histologically.

Results: The surface morphology of the scaffolds was analyzed via scanning electron microscopy (SEM). The surface of the EN PU scaffold showed random fiber structure and 3DP PCL scaffolds were stacked from multiple layers with PCL strands. The number of cells attached on to EN PU scaffold was higher than that on 3DP PCL scaffold. The outcome of implantation in vivo was successful, the defects of all groups were repaired by the graft without fistulas. Regeneration of submucous lamina propria was observed under the implanted scaffold in all four groups after implantation. Muscle regeneration might be more in the 3DP+hMSCs groups than in the EN+hMSCs groups. The thickness of the regenerated epithelium was significantly larger in naked EN- and hMSCs-seeded EN groups than that in the two 3DP groups. Neovascularization was significantly promoted in the two-inoculated groups than in the naked scaffold group, but the expression of macrophages was

higher in the naked scaffold groups (EN and 3DP) than in the hMSCs-treated groups.

Conclusion: Both EN PU scaffold and 3DP PCL scaffold showed successful regeneration. The tendency of more re-epithelization was found in EN PU scaffold and more muscle regeneration was found in 3DP PCL scaffold.

Keywords: esophagus, tissue engineering, regeneration, electrospinning, nanofiber, 3D printing, scaffold
Student number: 2017-21951

TABLE OF CONTENTS

LIST OF TABLES AND FIGURES

LIST OF ABBREVIATIONS

EN: Electrospun nanofiber

ECM: Extracellular matrix

3DP: 3-dimensional printing

PCL: Poly-caprolactone

PU: Polyurethane

SEM: Scanning electron microscope

hMSCs: Human adipose-derived mesenchymal stem cells

FN: Fibronectin

BUN: Blood urea nitrogen

WBC: White blood cell

HGB: Hemoglobin

ALB: Albumin

H&E: Hematoxylin and eosin

vWF: Von Willebrand factor

DAB: Diaminobenzidine

Introduction

Several medical conditions, such as congenital abnormality, esophageal cancer or trauma, necessitate surgical intervention, which results in esophageal defects. Therefore, the treatment for these conditions generally involve esophageal reconstruction. However, the conventional methods, reconstruction with the stomach, jejunum or colon, are invasive and can cause morbidities and mortality.[1,2] Hence, tissue engineering of an artificial esophagus that is similar to the native esophagus is emerging as an alternative.[3,4] Although tissue engineering may be a satisfactory and effective alternative strategy, a proper mimic of natural esophagus has not been developed so far. Lack of peristalsis after nondynamic scaffold implant can cause stenosis, graft obstruction, and anastomosis site leakage and subsequent sepsis. Occasionally, it also leads to death of the patient. Thus, the scaffolds should have characteristics of the native organ.

For successful esophageal reconstruction, selection of biomaterials is critical; an ideal material provides favorable environment for mucosal formation and esophageal muscle regeneration. Several types of artificial substitutes using synthetic materials have been researched for esophageal reconstruction.[5-9] Among various synthetic materials, electrospun polyurethane nanofibers have been

widely and successfully used, due to its advantages.[10] Electrospun nanofibers (EN), which is known to mimic human extracellular matrix (ECM), has shown excellent results in cell regeneration.[11] Additionally, nanofibers can be a promising option for esophageal tissue engineering because of their watertight properties and their resistance to bacterial invasion.[12]

And polycaprolactone (PCL) has reported its excellent mechanical strength and durability, and it is well compatible with 3-dimensional printing (3DP) systems.[13,14] A previous study reported that the mechanical properties of scaffolds built with 3DP technique enables them to withstand peristalsis and pressure.[15] The wide pores between the 3DP strands can provide a structural environment that is beneficial for esophageal muscle regeneration. In addition, human adipose-derived mesenchymal stem cells (hMSCs) have been reported for their usefulness in tissue regeneration, so have been used in several studies.[16-20]

Thus, with an aim to identify the ideal esophagus substitute, the purpose of this study was to evaluate the outcomes of esophageal reconstructions on rat model for partial esophageal defects using scaffolds made from 2 types of scaffolds with or without hMSCs seeding, respectively and to analyze the characteristics of each scaffolds.

Materials and methods

Preparation of EN scaffold and 3DP esophageal scaffold

The 3DP esophageal scaffold was fabricated using a rapid prototyping system.[15,21] The PCL (Sigma, USA) pellets were melted at 130° C in a heating chamber and 3DP strands were squeezed out by high pressure (~7 bar) using the Bioplotter® System (EnvisionTEC, Germany). A 3DP scaffold (1.5 × 2 mm) was plotted layer by layer with PCL bio ink extruded into cylinders. The diameter of the PCL strand was 150 μm and the thickness of the 3DP PCL scaffolds was 500 μm.

Electrospun esophageal scaffolds were fabricated by electrospinning technique. Briefly, The PU (Pellethane, Lubrizol, USA) pellets was stirred in N,N−dimethylformamide (Junsei Chemical Co., Japan) at room temperature for 10 hours to prepare a 20% (w/v) solution. PU solution was then filled in a syringe with 18G blunt tip needle and was electrospun using a high voltage power supply (Convertech; SHV200 RD−40k, Korea) at 15 kV potential between the needle tip and the stainless−steel collector (located on the ground) at room temperature. The feeding rate of the solution was fixed at 0.5 mL/hr. The electrically charged PU solution formed Taylor cone from the tip of the needle to the collector with a fixed working distance of 30 cm. The prepared EN scaffold was dried overnight in a vacuum oven (40 ° C) to

completely remove residual solvent. Prior to cell seeding, both scaffolds were sterilized by soaking in 70% ethanol under ultraviolet irradiation.

Morphological Analysis

The surface morphology of the EN PU scaffold and 3DP PCL scaffold were examined by scanning electron microscope (SEM; Model S-3000N; Hitachi, Japan). Surface and cross-section morphologies of the bilayer membrane were observed by a SEM operated at an accelerating voltage of 25 kV. The cross-sectional samples were prepared by cutting the membrane using a razor. Before the morphology observation, the patch specimens were coated with gold using a sputter coater under argon atmosphere. The fiber diameter and thickness of both the scaffolds were estimated by ImageJ software (NIH, USA) from the SEM micrographs.

Cell seeding and cellular viability

hMSCs (STEMPRO®, R7788-110), purchased from Gibco™), as model cells for transplantation were used. For efficient attachment on the surface of the 3DP scaffold, dissociated hMSCs were suspended in Matrigel (354234; Corning) at a density of 1×10^6 cells/mL. The Matrigel suspension containing the growth medium (MesenPRO RSTM, basal medium/growth supplement) was then

uniformly seeded on the surface of the 3DP scaffold. Separately, cell adhesion properties of EN scaffold was also enhanced by fibronectin (FN; BD Biosciences, USA) coating. FN-coated EN scaffolds were prepared by soaking the scaffolds in FN solution (1 mg/mL in PBS) at 37 ° C for 30 min. The FN-coated EN scaffolds were then rinsed with PBS and air dried for at least 1 hour at room temperature. The hMSCs were slowly inoculated at a density of 1 × 10^6 cells/mL on the surface of EN scaffold. The cells were allowed to adhere for 3 h and cultured in a growth medium for 2 or 5 days. Cell viability on the EN and 3DP scaffolds was evaluated after 5 days using a LIVE/DEAD® Viability Assay Kit (Molecular Probes, USA), according to the manufacturer' s instructions. Image capture was carried out with the Confocal Microscope's z-stack tool. Cell proliferation was determined on day 2 and 3 using CCK-8 assay (Dojindo, Japan). Briefly, 10% CCK-8 solution was added to each sample and maintained at 37° C for 2 hours. Aliquots from each sample (100 mL) were transferred to a 96-well plate and absorbance was measured at a wavelength of 450 nm using a Multiscan microplate reader (Thermo Scientific).

Surgical procedures

To assess the efficacy of EN and 3DP scaffolds for esophageal reconstruction, 8-week-old Adult Sprague-Dawley rats (Orient Bio, Seoul, Korea) were used. The animals were divided into four groups (n=7 per group) as follows: 1) implantation of the 3DP PCL

scaffold (3DP PCL); 2) implantation of hMSCs-seeded 3DP scaffolds (3DP+hMSCs); 3) implantation of the EN PU scaffold (EN PU); 4) implantation of hMSCs-seeded EN scaffolds (EN+hMSCs). The surgical procedure was as follows. The rats were anesthetized by intramuscular injection of tiletamine/zolazepam (50 mg/g dose) and 2% xylazine hydrochloride (2 mg/ kg dose) and surgical site was sterilized with betadine and 70% ethanol for aseptic surgery. The rats were placed in a supine position with the neck extended. A vertical skin incision was made at the midline and the strap muscles were divided to isolate the tracheoesophageal structure. Following appropriate exposure of the cervical esophagus under a magnified view, and the upper part was isolated from the thyroid gland carefully. A 1.5 × 2 mm wedge-shaped esophageal defect (about one thirds of circumference) including all layers was made using a scalpel. The partial esophageal defects in the rats of different groups were orthotopically reconstructed by the respective scaffold with a 9-0 nylon suture (Johnson & Johnson Co., Norderstedt, Germany) under a microscope. The muscle and skin tissues were then closed with a 4-0 Vicryl suture. Following the operation, Dextrose saline and water was given for 2 days. Oral liquid feeding (nutrition formula: 20.6 g / 100 mL [g%] carbohydrate, 3.8 g% protein, 0.2 g% fat) begins on the third post-operative day. Normal feeding was started 14 days after the procedure. All protocols and experimental design in this animal study were implemented according to the guideline of the Institutional Animal Care and Use

Committee of the Seoul National University Hospital (approval number: 17-0164-S1A0).

Evaluation of the postoperative clinical course and blood parameters

Postoperative monitoring was performed daily. The survival rate and weight of the animals were noted to assess the incidence of respiratory and surgical complications. In addition, experimental rats were also examined through the indicators of appearance and attitude, according to the 5-point scale (Table 1). All rats were sacrificed 4 weeks postoperation through the CO_2 inhalation. To monitor hydration status, anemia, and infection among experimental rats, we collected blood samples in ethylenediamine tetra-acetic acid anticoagulant bottles on the 1st and 4th postoperative weeks. Essential blood parameters [blood urea nitrogen (BUN), white blood cells (WBCs), hemoglobin (HGB), albumin (ALB)] were investigated in the experimental groups (n=5). Biochemical tests (BUN and ALB) were performed using a Hitachi 7180i Autoanalyzer (Hitachi High-Technologies Corporation, Japan). The complete blood count (WBC and HGB) was analyzed using a hematology autoanalyzer-ADVIA2120i (Siemens Healthcare Diagnostics Inc., USA). All tests were performed within 30 minutes of collection.

Radiological and histological examination

A micro-CT scanner (NFR Polaris-G90, Nanofocusray, Korea) was used to check saliva leakage from esophageal defect. Prior to the CT scan, all rats have performed oral injection of barium sulfate (Solotop HD, Tae Joon Pharm. Co., Ltd.), a contrast agent. Three-dimensional images of rat esophagus were obtained and reconstructed (Lucion, Infinitt Healthcare, Korea). All experimental rats were sacrificed after the radiological examination.

Esophageal tissue including the implanted site were fixed in 10% neutral-buffered formalin, embedded in paraffin, and cut into 4 μm thick sections. The sections were deparaffinized and dehydrated in a graded series of ethanol. The tissue slides were then stained with hematoxylin and eosin (H&E) and Masson's trichrome, following standard histological procedure. Elastin staining was also performed using the Elastic (Modified Verhoff's) stain Kit (ES4807), according to the manufacturer's instructions. Histological images were captured in triplicate for each group using a light microscope (Olympus, Japan).

Immunohistological analysis

For immunohistochemistry, tissue samples were soaked in 3% hydrogen peroxide (H_2O_2) in methanol for 30 min to inactivate endogenous peroxidase. The tissue slides were rinsed with PBS and then were incubated to 3% bovine serum albumin to block nonspecific response. The tissue sections were subsequently reacted with anti-desmin (1:200 dilution; rabbit polyclonal antibody; Abcam, UK) and anti-keratin 13 (1:50 dilution; mouse monoclonal antibody; ABIN126702) along with the secondary antibodies Alexa Fluor 488 goat anti-rabbit (ab150077; Abcam, UK) and Alexa Fluor 594 goat anti-mouse (ab150116; Abcam, USA), respectively. Desmin$^+$ fluorescence was calculated from green-positive area around the implanted site using ImageJ software (n=5). The thickness of regenerated esophageal epithelium was also measured using ImageJ software (n=5). Tissue sections for Von Willebrand factor (vWF, 1:200 dilution; rabbit monoclonal antibody; Abcam, UK) and CD68 (1:100 dilution; mouse monoclonal antibody; Abcam, UK) were subsequently incubated using the horseradish peroxidase-conjugated kit (Vectastain®), and they were visualized using chromogenic substrate 3,3' diaminobenzidine (DAB; Vector, pk-7800). Cell nuclei were counterstained with hematoxylin. Histological images were obtained using a fluorescence microscope (BX43-32FA1-S09; Olympus Optical, Japan). The number of vWF-positive vessels and CD68-

positive cells was calculated using ImageJ. Five areas (200× magnification) were analyzed per slide (n = 5 per group) by a blinded observer.

Statistical analysis

The data are expressed as the means ± standard deviation. Statistical significance was determined via one-way analysis of variance (ANOVA) with Tukey-Kramer's post hoc test (GraphPad Prism 5, GraphPad Software, La Jolla, CA). Statistical significance was marked as * ($P < 0.05$), ** ($P < 0.01$), and ***($P < 0.001$).

Results

Surface morphology and cytotoxicity of esophageal scaffolds

The surface morphology of the two types of esophageal scaffolds was analyzed using SEM (Figure 2). The surface of the EN scaffold showed fiber structure with an average diameter of ~800nm, arranged randomly, resembling the native ECM structures. In contrast, in 3DP scaffolds, microscale PCL strands of 150 μm diameter were stacked up to form multiple layers.

Cytotoxicity of EN and 3DP scaffolds was assessed by Live & dead stain and CCK-8 assay after three-dimensional culture of inoculated hMSCs. After uniformly attaching of hMSCs to each patch scaffold, the cells were monitored for 5 days. In the EN scaffold, most of the cells survived and did not exhibit alignment along any orientation; however, in the 3DP scaffold the cells were found to be aligned along the PCL strands (Figure 3). The number of attached cells in the EN scaffold were higher than that in the 3DP scaffold. Meanwhile, CCK-8 assay revealed that both the groups showed a significant increase in proliferation of hMSCs (Figure 4).

Orthotopic esophageal implantation and postoperative outcomes

Each patch scaffolds were implanted at partial esophageal defect site under microscopic magnification (Figure 5). All of the experimental rats survived but their body weight decreased rapidly

within one week (Figure 6). However, their body weight increased gradually, and after 4 weeks, the animals showed complete recovery in their body weight. In addition, there was no leakage of saliva after implantation, and no significant weight difference between groups were observed. The physical condition of the animals was quantified by the animal's appearance and attitude scoring system (Figure 7). The grading score was significantly higher at 4 weeks than that at 1 week for both parameters in all groups. In terms of functionality, micro-CT analysis confirmed that there was no leakage of orally injected contrast agent in the entire esophagus (Figure 8). These results showed that partial esophageal defects were regenerated by the graft without fistulas.

Blood parameters

Blood tests, including BUN, WBC, HGB, and ALB were conducted at 1 and 4 weeks after implantation (Figure 9). BUN, which is related to dehydration was significantly increased at week 4 rather than week 1 in all experimental groups. The WBC also found to be decreased in all groups during this period. These could be due to a gradual decline in inflammatory response after implantation. HGB, which is associated with anemia, was significantly increased at week 4 compared to week 1 in all the groups. ALB increased slightly in the experimental groups at weeks 4 but did not show a statistical difference.

Histological evaluation at implanted sites

Whole histology of the esophageal grafts including EN PU, EN + hMSCs, 3DP PCL and 3DP + hMSCs scaffolds was confirmed by H&E staining. The implanted scaffolds had completely covered the regenerated esophageal lumen in the defect site (Figure 10A). Figure 10B shows regeneration of submucous lamina propria, the blue color of Masson's trichrome staining indicates collagen deposition at esophageal lamina propria, under the implanted scaffold in all four experimental groups. Distribution of elastin fibers, which influence the elastic properties of the esophagus, were examined through elastin staining (Figure 11).

Regeneration of esophageal muscle and epithelium

Desmin immunostaining was performed to examine the implanted scaffolds and determine whether hMSCs-seeding helped in the regeneration of esophageal muscle around the implanted site. Strong green colors were seen near the implanted EN (white dot line) and 3DP (marked by a white star) scaffolds (Figure 12). Desmin-positive area was significantly wider in the 3DP+hMSCs group compared to the EN+hMSCs group (Figure 13). It might be represented that esophageal muscle regenerated more of the the 3DP+hMSCs group than EN+hMSCs group. Regeneration of the esophageal mucosa at 4 weeks after transplantation was identified by keratin13 immunostaining. Figure 14 shows the connectivity of the esophageal epithelium at the defect site, as indicated in red

color. NakedEN and hMSCs-seeded EN groups increased the thickness of regenerated epithelium significantly more than the corresponding 3DP groups (Figure 15).

Neovascularization and inflammatory responses in the implanted sites

Immunostaining for vWF, an endothelial marker was carried out to identify the newly formed blood vessels at the implanted sites of each group (Figure 16). Newly formed vessels were found to be abundant at the implanted site (black arrows). Neovascularization was significantly promoted in the two hMSCs-inoculated groups than in the naked scaffold (EN and 3DP) groups (Figure 17). CD68 immunostaining for macrophage infiltration at the transplanted site is shown in Figure 18. Expression of macrophages (DAB-positive stains; brown color) at week 4 was higher in the naked scaffold groups (EN & 3DP) than in the hMSCs-treated groups (Figure 18). These results suggest that hMSCs provides immunomodulatory function on esophageal reconstruction.

Discussion

The esophagus is a multi-layered organ, consisting of the mucosal, submucosal, muscularis, and adventitial layers, without ability to regenerate. Therefore, to treat large structural defects in the esophagus, primary repair or esophageal reconstruction with gastric pull up technique with jejunum or colon has been employed traditionally.[5,6] However, such simple repairs and conventional reconstruction procedures associated with a high risk of failure due to fatal complications and morbidity. Thus, artificial grafts similar to esophageal tissues, made using tissue engineering and regenerative medicine have emerged as alternatives, and various materials have been used.[22,23] The ideal artificial esophagus should be resistant to the low pH environment caused by gastric acid, and it should not cause infection, inflammation, or stenosis, and promote the proliferation of cells in the scaffold. At the same time, substitute of esophagus should have the strength and stability to endure the pressure from a food bolus and elasticity to synchronize peristalsis with the gastrointestinal tract.[24]

Although there have been several studies on esophageal reconstruction with various materials, previous studies have not been successful due to several factors. An acellular matrix without cell seeding, polyethylene plastic and silicon, did not improve

regeneration of epithelium, resulting in the failure of esophageal reconstruction by infection or narrowing.[24,25] Several studies on xenografts and decellularized and matured esophageal scaffolds have revealed excellent regeneration results, but these have weak mechanical properties, and are difficult to commercialize because of the high risk of disease transmission and immune-related disadvantages.[26,27] The failure of reconstruction with the scaffold by leakage, and necrosis often leads to mediastinal and cervical contamination and inflammation, and is also associated with high mortality. The regeneration of mucosal epithelium is important in avoiding inflammation and stenosis and the reproduction of muscle cells is important to restore of function of the esophagus. For these reasons, recent research has focused on proliferating and regenerating mucosal epithelial cells as well as reproducing the mechanical strength of native esophagus by rebuilding smooth muscle cells.[28]

Ghasemi-Mobarakeh et al. have presented a study on electrospinning and showed that it is suitable to make scaffolds that closely mimics human ECM. However, scaffolds made of EN have weak mechanical properties, and so have limitations as artificial esophagus.[11] On the other hand, recent studies on the production of scaffolds using 3DP have shown that the method can produce various tissue structures by constructing biomaterials in a layer by layer fashion and can accurately reproduce them.[29] In previous studies reported that 3DP strands can provide adequate mechanical

strength and flexibility for normal functioning of esophagus.[15] In the present study, our SEM results showed that EN PU scaffolds formed random fiber structures, similar to native ECM, and the PCL strands in the 3DP PCL scaffold formed multilayered structures. Our observations were similar to those reported by others.[15,28] In cytotoxicity of EN PU and 3DP PCL scaffolds, there was a significant increase in proliferation of hMSCs, as seen by CCK-8 assay on both groups, suggesting that both EN PU and 3DP PCL could infiltrate the cells into scaffolds and promote proliferation, and the number of attached cells of EN PU scaffolds was higher than that of 3DP PCL scaffolds and this result makes it possible to assume that EN PU scaffolds may be suitable for cell regeneration. However, this result should be interpreted very carefully, because both synthetic materials and fabrication methods are different, it is unclear which effect is significant. Further study is needed to determine how these materials, PU and PCL, and fabrication methods, EN and 3DP, affect tissue regeneration, respectively.

Because many important major organs are present in the mediastinum and neck, contamination by reconstruction failure results in severe morbidity and complication.[30] In the present study, during the second week after surgery, feeding was limited, which was intended for stable engraftment of the scaffold. This resulted in worsening of physical condition, represented by a low value in appearance and attitude scores during that period and weight loss. However, after 4 weeks of operation, the physical condition was

significantly improved compared to condition after the first week, and the body weight of animals in the experimental groups gradually recovered and eventually restored the preoperative level. Similar to the results of our study, Lopes et al. performed a repair of partial esophageal defects in rat model with small intestinal submucosa patch grafts and showed no signs of esophageal dysfunction and return of normal weight of the animals after the treatment.[31]

The absence of fistulas and leakages in the reconstructed esophagus was demonstrated not only by improvements in the general condition of the experimental group, but also by micro-CT analysis with orally injected contrast agent and 3D reconstruction. And, histologically, we could observe that the lumen defects of all groups were sufficiently regenerated with scaffold implantation. The epithelial cells and the submucous lamina propria under scaffolds were successfully regenerated in all experimental groups. In particular, the morphology of elastin deposits in the EN + hMSCs and 3DP + hMSCs groups was very similar to that of normal esophagus. And it is important that the implanted scaffold provides adequate physical support for esophageal peristalsis. In several studies, artificial scaffolds have sufficient modulus of elasticity and maximum stress compared with native esophagus.[15] However, it is difficult to for synthetic materials to mimic real muscle elasticity, and there is a need to study materials such as collagen and elastin to mimic the esophageal peristalsis and its mechanical properties. In the present study, the presence of rich elastin components might

performed an important role in improving the mechanical properties of the esophagus.

Several studies have reported on the efficacy of hMSCs for tissue regeneration.[32,33] And hMSCs have been reported to be able to differentiate into cells of mesengenic lineage, such as smooth muscle cells, chondrocytes, adipocytes, and osteoblasts.[34,35] Kim et al. reported that hMSCs exerts a paracrine effect to regulate the microenvironment for promoting tissue regeneration. This is due to various cytokines, growth factors, and ECM that hMSCs produce.[36] Although the mechanism is not clearly understood, the immunosuppressive effects of hMSCs have been used in several animal models.[16,18] hMSCs may be important in tissue generation because they have immune privilege and immunomodulatory effects, which seem to be related to that of paracrine.[17,19,20,37] Based on the theories and studies mentioned above, we used hMSCs in this study. As expected, in all hMSCs-seeded scaffolds group, the morphology of elastin closely resembled the native esophagus, and neovascularization was significantly increased. Moreover, hMSCs seemed to have provided immune regulatory function. However, in this study, the method of seeding hMSCs on each scaffold was different. FN coating method was used for EN PU scaffold and the Matrigel suspension containing the growth medium was used for 3DP PCL scaffold, therefore, further study is needed to determine the effect of this difference.

As shown in Figure 7, the experimental rats recovered their

weight after one month of surgical procedure and these results were also reflected in the blood parameters. BUN is known to be related in animal dehydration.[38] In the present study, BUN of all groups increased significantly, and physical conditions of all experiments improved over the period of 4 weeks. However, WBC, an inflammation-related blood parameter, decreased significantly in all groups. Moreover, the HGB value significantly increased during this period in all experimental groups indicating no anemia, which is also closely related to malnutrition.[39] Therefore, these findings suggest that the implantation was successful, and thus, despite dehydration, the subjects overcame inflammation and malnutrition.

Re-epithelialization is closely related to the prevention of infection, granulation tissue formation and stenosis, and smooth muscle regeneration plays a major role in providing esophageal function, especially peristalsis and mechanical strength. Regeneration of both type of tissues is crucial for esophageal reconstruction, but many previous studies were primarily concerned with the regeneration of mucosal epithelium, which did not fully account for the multi-layered esophageal structures containing both epithelium and muscle.[24,25] Park et al. reported that a 3DP scaffold can be used to create a multi-layered artificial esophagus with smooth muscle regeneration.[28] In the present study, muscle regeneration, less than normal esophagus, and sufficient epithelial regeneration were observed in all types of scaffolds, it was assumed that the structural environment of the 3DP PCL scaffold

might have been effective in muscle regeneration and that ECM-like properties of the EN PU scaffold had a structural effect in improving re-epithelialization. From these results, we hypothesize that, in order to reproduce the multi-layer structure of the esophagus, using the properties of these two types of scaffolds to design complex substitutes could closer to ideal esophageal reconstruction. However, these results should be taken carefully, since desmin is a subunit of intermediate filaments in both skeletal muscle and smooth muscle tissue, immunostaining of desmin alone cannot able to distinguish between regenerated muscles and the muscles around the esophagus.[40]

There are several limitations in the present study. First, there are many factors, fabrication method, synthetic material, and hMSCs seeding method, in each types of scaffolds, so it is difficult and unclear to assess their respective effects. Therefore, further studies are needed to assess the individual effects of each factors. And this study only focused on the reconstruction of partial defects in the esophagus. The reconstruction of circumferential defects is still a challenging part of esophageal reconstruction in animal model, most of which are clinically serious and important. Research on reconstruction for circumferential defects and longer defects will be needed in the future. Moreover, the results of this experiment were evaluated only for a short-term outcome, 4 weeks after surgery. Therefore, long-term studies with more animals will be needed in the future. Before its clinical application, the mechanical properties

of the scaffold should be improved to mimic original esophagus, and additional methods should be established to facilitate tissue regeneration.

Conclusions

In conclusion, both EN PU scaffold and 3DP PCL scaffold showed successful regeneration. The tendency of more re-epithelization was found in EN PU scaffold and more muscle regeneration was found in 3DP PCL scaffold. Further research will be needed to reconstruct the circumferential defects in the rat model and in the larger animal models.

References

1. Irino T, Tsekrekos A, Coppola A, et al. Long-term functional outcomes after replacement of the esophagus with gastric, colonic, or jejunal conduits: a systematic literature review. *Dis Esophagus.* 2017;30(12):1-11.
2. Flanagan JC, Batz R, Saboo SS, et al. Esophagectomy and Gastric Pull-through Procedures: Surgical Techniques, Imaging Features, and Potential Complications. *Radiographics.* 2016;36(1):107-121.
3. Catry J, Luong-Nguyen M, Arakelian L, et al. Circumferential Esophageal Replacement by a Tissue-engineered Substitute Using Mesenchymal Stem Cells: An Experimental Study in Mini Pigs. *Cell Transplant.* 2017;26(12):1831-1839.
4. Wang F, Maeda Y, Zachar V, Ansari T, Emmersen J. Regeneration of the oesophageal muscle layer from oesophagus acellular matrix scaffold using adipose-derived stem cells. *Biochem Biophys Res Commun.* 2018;503(1):271-277.
5. Poghosyan T, Gaujoux S, Sfeir R, Larghero J, Cattan P. Bioartificial oesophagus in the era of tissue engineering. *J Pediatr Gastroenterol Nutr.* 2011;52 Suppl 1:S16-17.
6. Shen Q, Shi P, Gao M, et al. Progress on materials and scaffold fabrications applied to esophageal tissue engineering. *Mater Sci Eng C Mater Biol Appl.* 2013;33(4):1860-1866.
7. Tan JY, Chua CK, Leong KF, Chian KS, Leong WS, Tan LP. Esophageal tissue engineering: an in-depth review on scaffold design. *Biotechnol Bioeng.* 2012;109(1):1-15.
8. Mecozzi A, Matera F. Polarization scattering by intra-channel collisions. *Opt Express.* 2012;20(2):1213-1218.
9. Aaltonen T, Abazov VM, Abbott B, et al. Evidence for a particle produced in association with weak bosons and decaying to a bottom-antibottom quark pair in higgs boson searches at the tevatron. *Phys Rev Lett.* 2012;109(7):071804.
10. Kilic E, Yakar A, Pekel Bayramgil N. Preparation of electrospun polyurethane nanofiber mats for the release of doxorubicine. *J Mater Sci Mater Med.* 2017;29(1):8.
11. Ghasemi-Mobarakeh L, Prabhakaran MP, Morshed M, Nasr-Esfahani MH, Ramakrishna S. Electrospun poly(epsilon-caprolactone)/gelatin nanofibrous scaffolds for nerve tissue engineering. *Biomaterials.* 2008;29(34):4532-4539.
12. Ziegler A, Schneider A, Pittman A, Thorpe E. Postoperative Tachycardia in Head and Neck Microvascular Free Flap Patients. *Otolaryngol Head Neck Surg.* 2019;160(6):1019-1022.
13. Dash TK, Konkimalla VB. Poly-small je, Ukrainian-caprolactone based formulations for drug delivery and tissue engineering: A review. *J Control Release.* 2012;158(1):15-33.
14. Park S, Kim G, Jeon YC, Koh Y, Kim W. 3D polycaprolactone

scaffolds with controlled pore structure using a rapid prototyping system. *J Mater Sci Mater Med.* 2009;20(1):229-234.
15. Kim IG, Wu Y, Park SA, et al. Tissue-Engineered Esophagus via Bioreactor Cultivation for Circumferential Esophageal Reconstruction. *Tissue Eng Part A.* 2019.
16. Lee SY, Kwon B, Lee K, Son YH, Chung SG. Therapeutic Mechanisms of Human Adipose-Derived Mesenchymal Stem Cells in a Rat Tendon Injury Model. *Am J Sports Med.* 2017;45(6):1429-1439.
17. Li CL, Leng Y, Zhao B, et al. Human iPSC-MSC-Derived Xenografts Modulate Immune Responses by Inhibiting the Cleavage of Caspases. *Stem Cells.* 2017;35(7):1719-1732.
18. Liu X, Chen W, Zhang C, et al. Co-Seeding Human Endothelial Cells with Human-Induced Pluripotent Stem Cell-Derived Mesenchymal Stem Cells on Calcium Phosphate Scaffold Enhances Osteogenesis and Vascularization in Rats. *Tissue Eng Part A.* 2017;23(11-12):546-555.
19. Marigo I, Dazzi F. The immunomodulatory properties of mesenchymal stem cells. *Semin Immunopathol.* 2011;33(6):593-602.
20. Nauta AJ, Fibbe WE. Immunomodulatory properties of mesenchymal stromal cells. *Blood.* 2007;110(10):3499-3506.
21. Lee SJ, Heo DN, Park JS, et al. Characterization and preparation of bio-tubular scaffolds for fabricating artificial vascular grafts by combining electrospinning and a 3D printing system. *Phys Chem Chem Phys.* 2015;17(5):2996-2999.
22. Kim SH, Lee KS, Shim YM, Kim K, Yang PS, Kim TS. Esophageal resection: indications, techniques, and radiologic assessment. *Radiographics.* 2001;21(5):1119-1137; discussion 1138-1140.
23. Wormuth JK, Heitmiller RF. Esophageal conduit necrosis. *Thorac Surg Clin.* 2006;16(1):11-22.
24. Kuppan P, Sethuraman S, Krishnan UM. Tissue engineering interventions for esophageal disorders--promises and challenges. *Biotechnol Adv.* 2012;30(6):1481-1492.
25. Totonelli G, Maghsoudlou P, Fishman JM, et al. Esophageal tissue engineering: a new approach for esophageal replacement. *World J Gastroenterol.* 2012;18(47):6900-6907.
26. Badylak SF, Vorp DA, Spievack AR, et al. Esophageal reconstruction with ECM and muscle tissue in a dog model. *J Surg Res.* 2005;128(1):87-97.
27. Luc G, Charles G, Gronnier C, et al. Decellularized and matured esophageal scaffold for circumferential esophagus replacement: Proof of concept in a pig model. *Biomaterials.* 2018;175:1-18.
28. Park SY, Choi JW, Park JK, et al. Tissue-engineered artificial oesophagus patch using three-dimensionally printed polycaprolactone with mesenchymal stem cells: a preliminary report. *Interact Cardiovasc Thorac Surg.* 2016;22(6):712-717.
29. Hong HJ, Chang JW, Park JK, et al. Tracheal reconstruction using chondrocytes seeded on a poly(L-lactic-co-glycolic acid)-

fibrin/hyaluronan. *J Biomed Mater Res A.* 2014;102(11):4142-4150.
30. Huang K, Wu B, Ding X, Xu Z, Tang H. Post-esophagectomy tube feeding: a retrospective comparison of jejunostomy and a novel gastrostomy feeding approach. *PLoS One.* 2014;9(3):e89190.
31. Lopes MF, Cabrita A, Ilharco J, et al. Esophageal replacement in rat using porcine intestinal submucosa as a patch or a tube-shaped graft. *Dis Esophagus.* 2006;19(4):254-259.
32. Lee DY, Kim HB, Shim IK, Kanai N, Okano T, Kwon SK. Treatment of chemically induced oral ulcer using adipose-derived mesenchymal stem cell sheet. *J Oral Pathol Med.* 2017;46(7):520-527.
33. Lee DY, Lee JH, Ahn HJ, et al. Synergistic effect of laminin and mesenchymal stem cells on tracheal mucosal regeneration. *Biomaterials.* 2015;44:134-142.
34. Gong Z, Niklason LE. Use of human mesenchymal stem cells as alternative source of smooth muscle cells in vessel engineering. *Methods Mol Biol.* 2011;698:279-294.
35. Phinney DG, Prockop DJ. Concise review: mesenchymal stem/multipotent stromal cells: the state of transdifferentiation and modes of tissue repair--current views. *Stem Cells.* 2007;25(11):2896-2902.
36. Kim M, Kim KH, Park SR, Choi BH. Mesenchymal stem cells for treatment of neurological disorders: a paracrine effect. *Tissue Engineering and Regenerative Medicine.* 2013;10(5):234-245.
37. Salamon A, Toldy E. The role of adult bone marrow derived mesenchymal stem cells, growth factors and carriers in the treatment of cartilage and bone defects. *J Stem Cells.* 2009;4(1):71-80.
38. Yoshihara A, Hirotomi T, Takano N, Kondo T, Hanada N, Miyazaki H. Serum markers of chronic dehydration are associated with saliva spinability. *J Oral Rehabil.* 2007;34(10):733-738.
39. Sinha N, Mishra TK, Singh T, Gupta N. Effect of iron deficiency anemia on hemoglobin A1c levels. *Ann Lab Med.* 2012;32(1):17-22.
40. Li Z, Mericskay M, Agbulut O, et al. Desmin is essential for the tensile strength and integrity of myofibrils but not for myogenic commitment, differentiation, and fusion of skeletal muscle. *J Cell Biol.* 1997;139(1):129-144.

Table

Score	Appearance	Attitude
5	Normal; normal skin tent and posture	Normal; active in cage prior to and during handing
4	Skin tent present on dorsum	Decreased activity, but alert, responsive to handling
3	Hunched posture, piloerection present, moderate skin tent	Lethargic, decreased resistance to handing
2	Eyes sunken in, piloerection and skin tent severe	Nonresponsive mouse only moves when touched
1	Failure to right itself	Failure to flee when hand is presented in cage

Table 1. Appearance and Attitude Scales

Figures

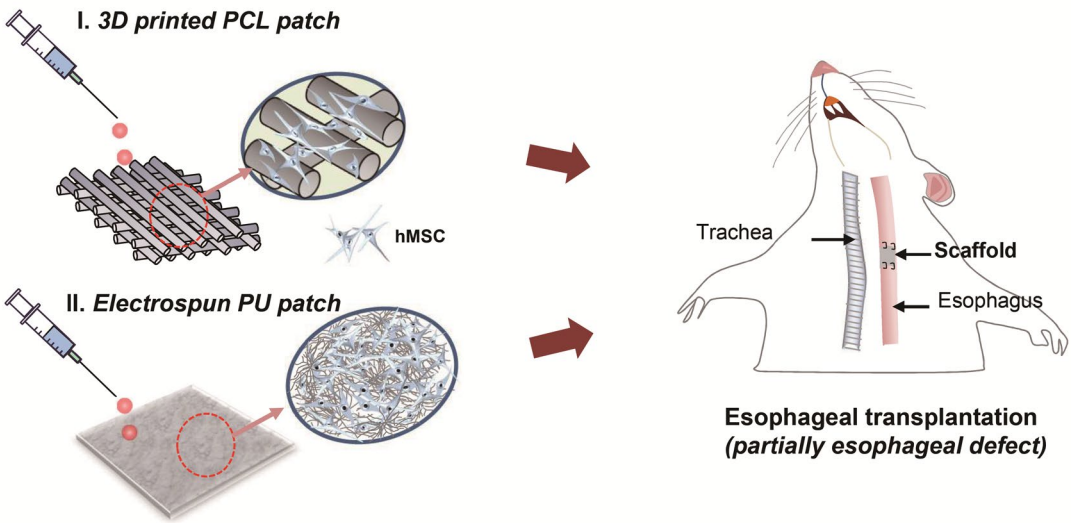

Figure 1. Schematic diagram showing the pre-seeding of hMSCs on the surface of 3DP patch and EN patch in vitro, and the implantation of each scaffold onto the partial esophageal defect of rat.

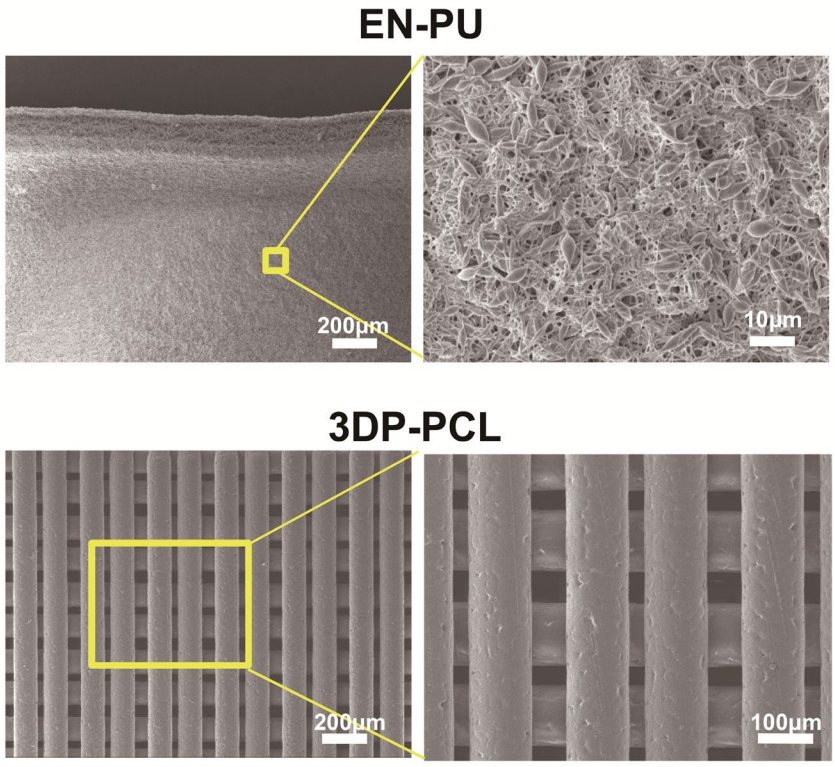

Figure 2. SEM photographs of the EN PU patch and 3DP PCL patch.

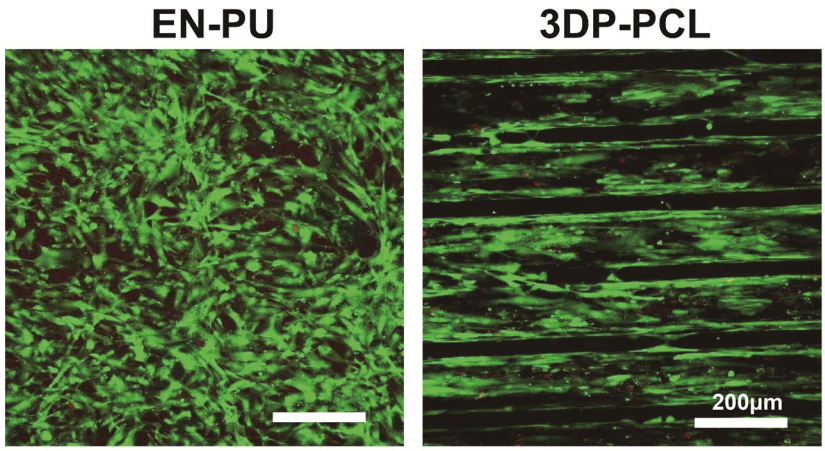

Figure 3. Live/dead staining to analyze cell viability on each scaffold.

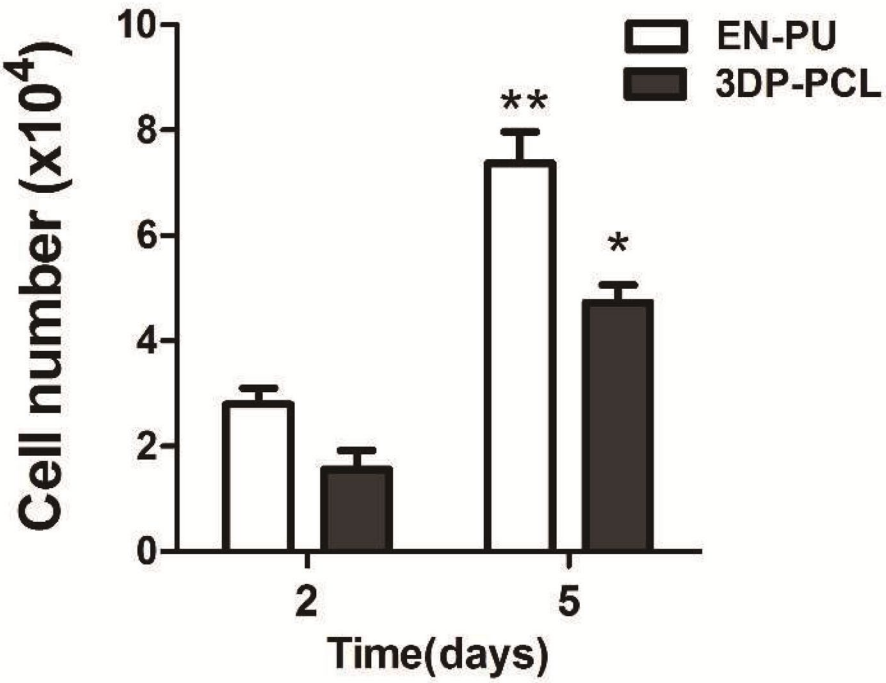

Figure 4. hMSCs proliferation on surface of each scaffold at days 2 and 5 via the CCK-8 metabolic assay.

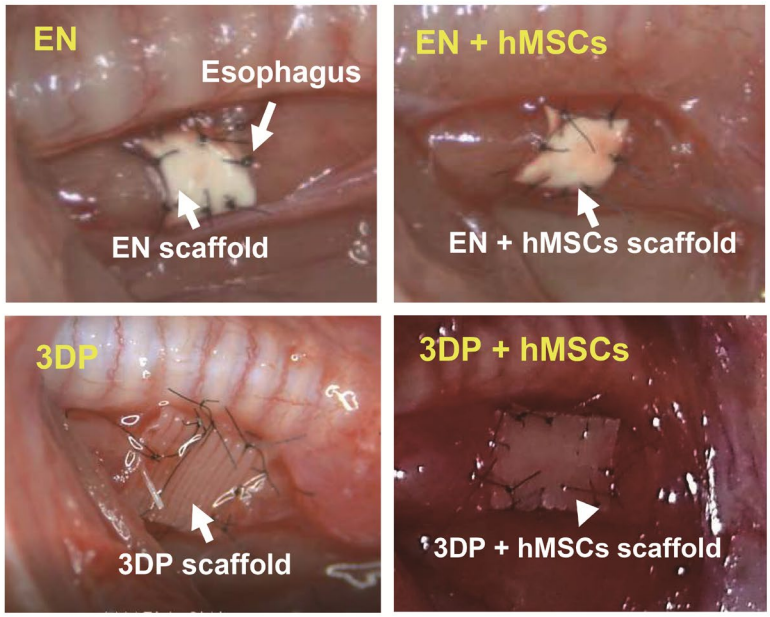

Figure 5. Each patch scaffold was transplanted onto the full thickness esophageal partial defect of rat model.

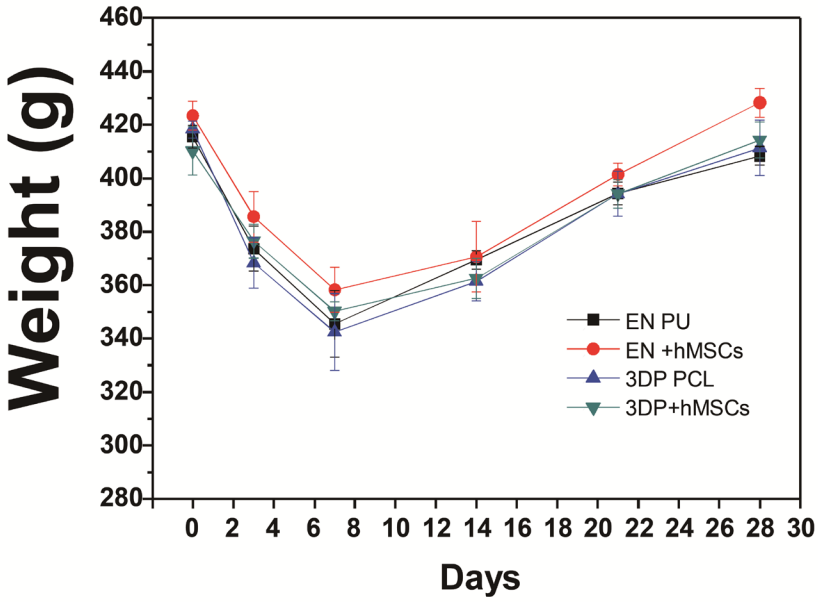

Figure 6. Weight change of the animals.

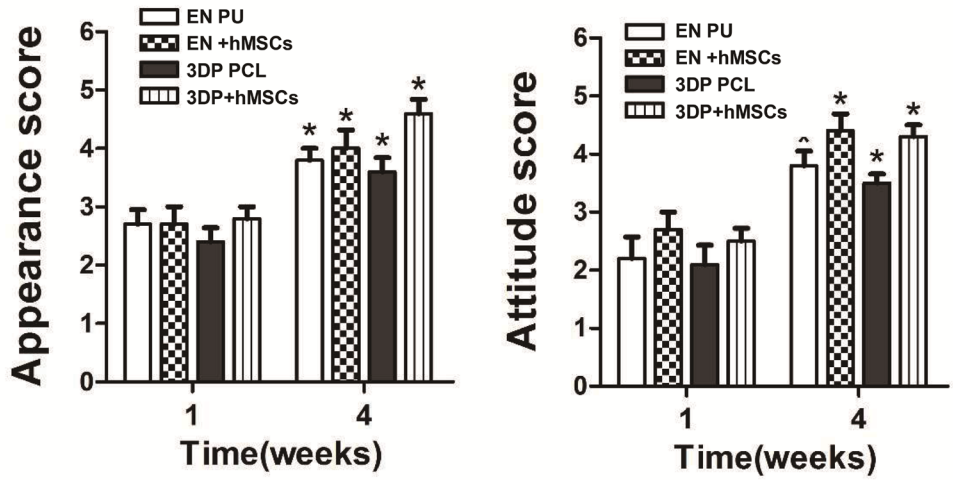

Figure 7. Postoperative physical condition of the animals assessed by scores of attitude and appearance.

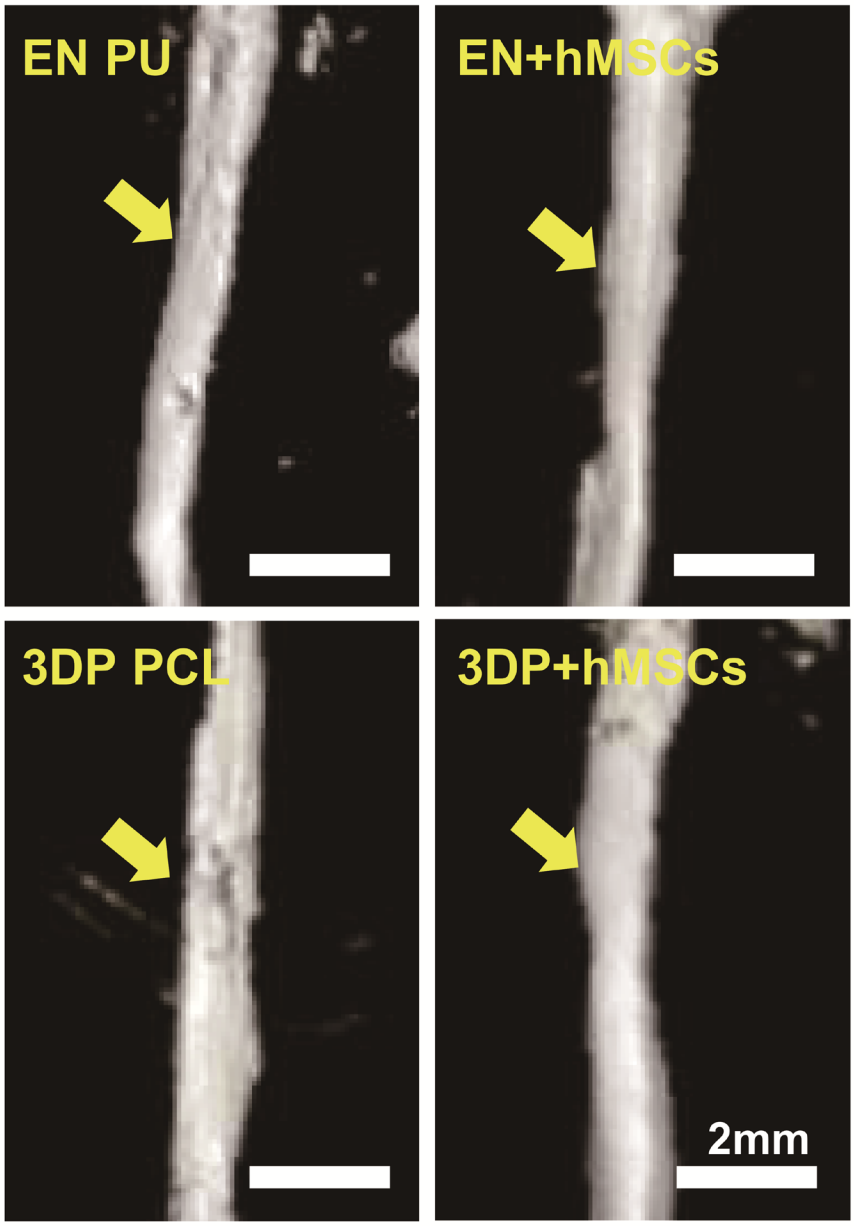

Figure 8. Micro CT images of the implanted site (yellow arrow) from each group. Esophageal fistulas were not observed.

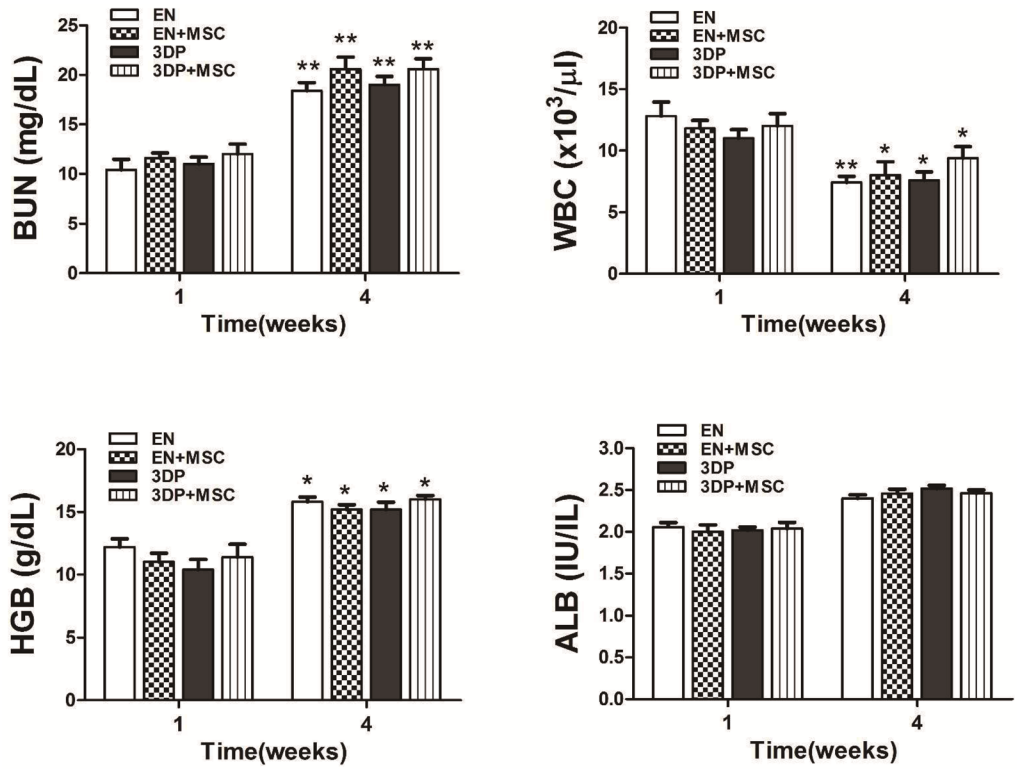

Figure 9. Postoperative blood parameters.

*. $p < 0.05$

**. $p < 0.01$

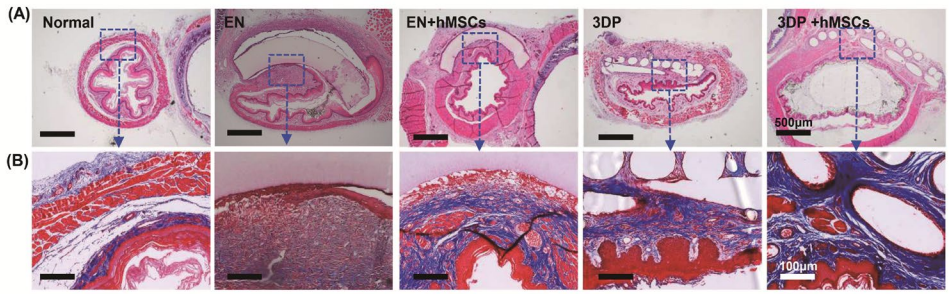

Figure 10. (A) Whole histology of the reconstructed esophagus 4 weeks after implantation of each scaffold. (B) Collagen deposition around the implanted sites for each group with Masson's trichrome staining.

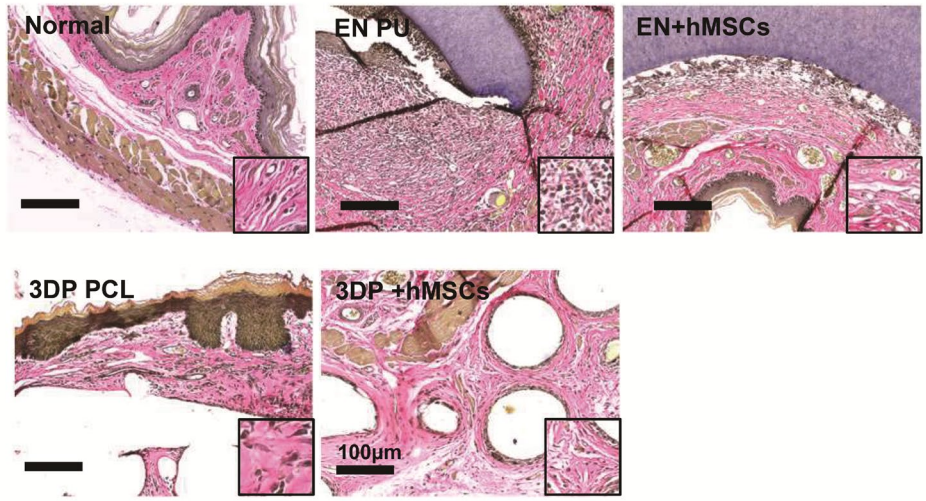

Figure 11. The regeneration of elastin fiber confirmed by elastin immunostaining.

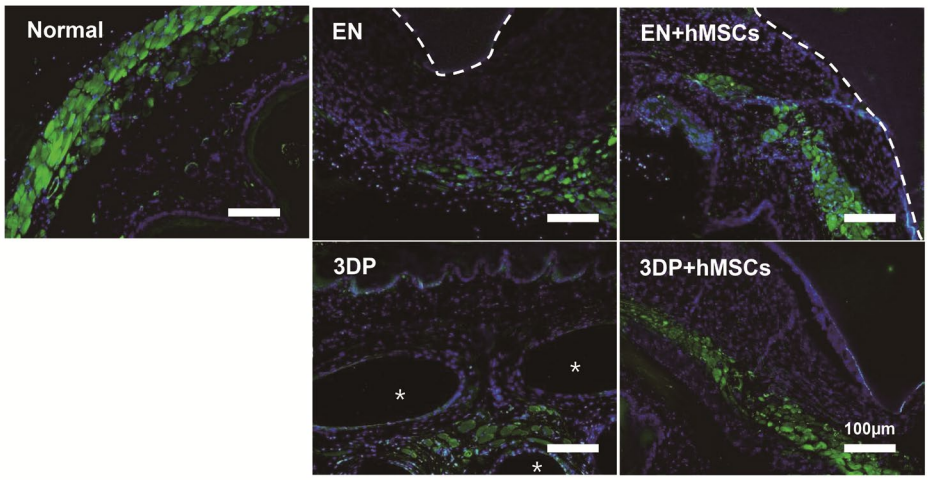

Figure 12. Representative images of desmin immunostaining (green colors) in the reconstructed esophagus after scaffold implantation (white dot line, EN fiber; *, 3DP strand).

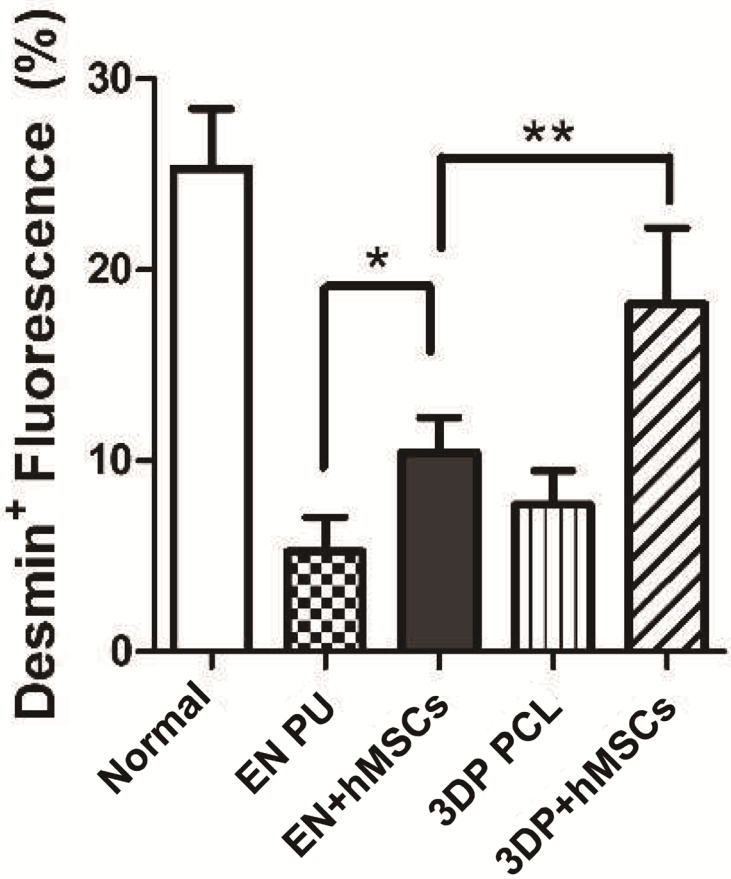

Figure 13. Quantitative analysis of the desmin-positive area

*. $p < 0.05$

**. $p < 0.01$

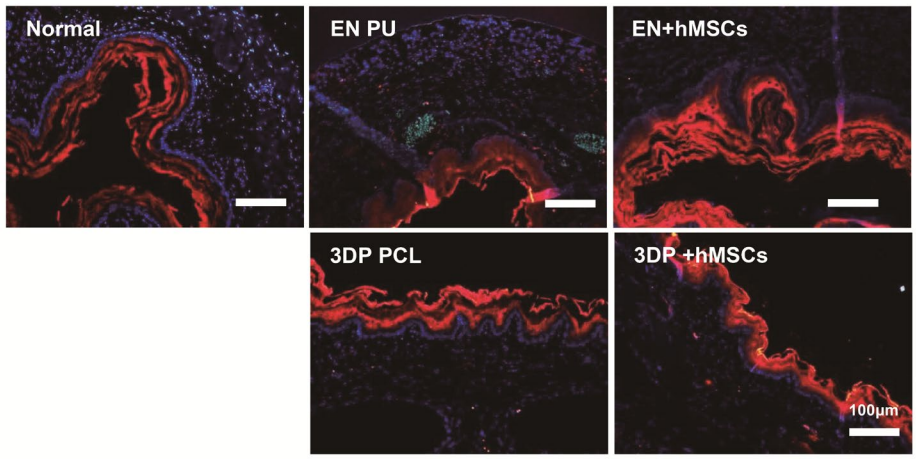

Figure 14. Keratin-13 immunostaining regenerative esophageal epithelium at 4 weeks after implantation (red colors).

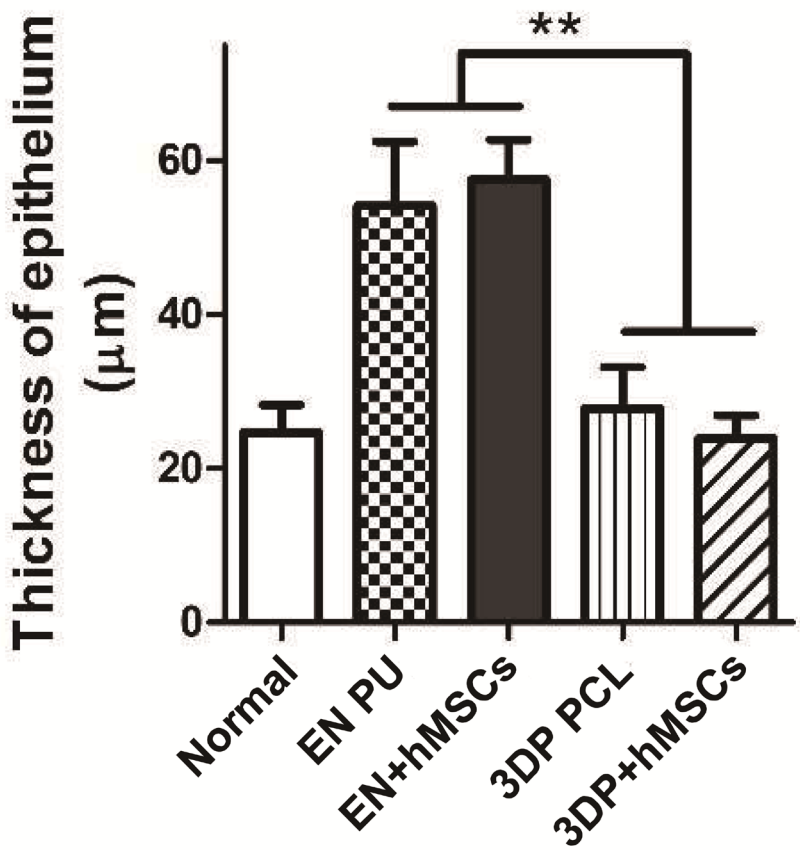

Figure 15. Quantitative analysis of the re-epithelialization 4 weeks after the surgery.

**. $p < 0.01$

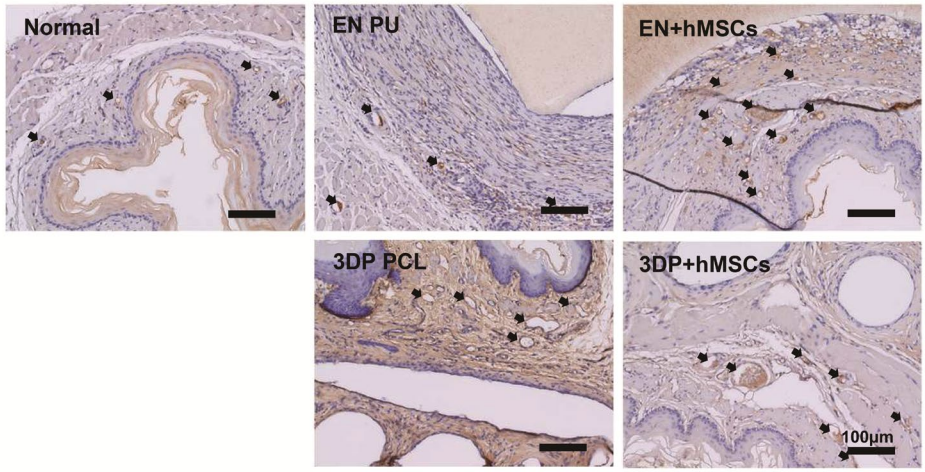

Figure 16. Immunohistochemical staining of neovascularization at 4 weeks after implantation. Representative images showing the newly formed blood vessels by Von Willebrand factor (vWF) expression. (Black arrows, vWF-positive vessels.)

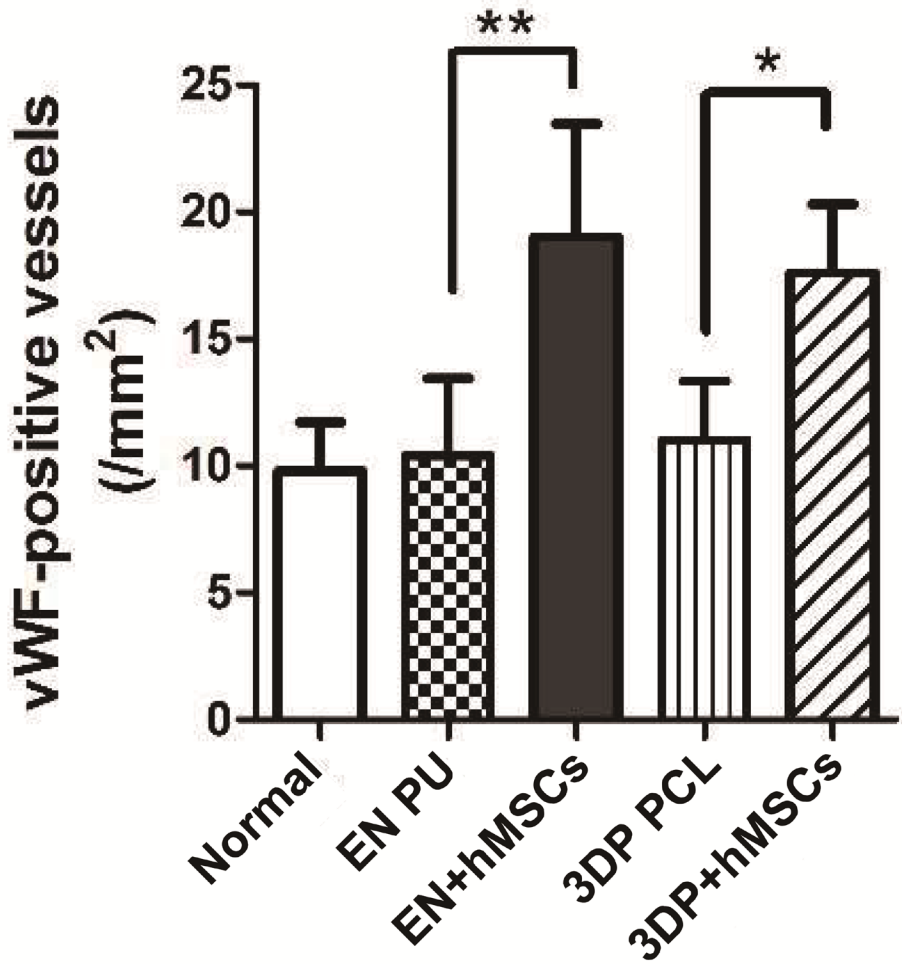

Figure 17. Statistical analysis of the number of vWF-positive blood vessels per square millimeter.

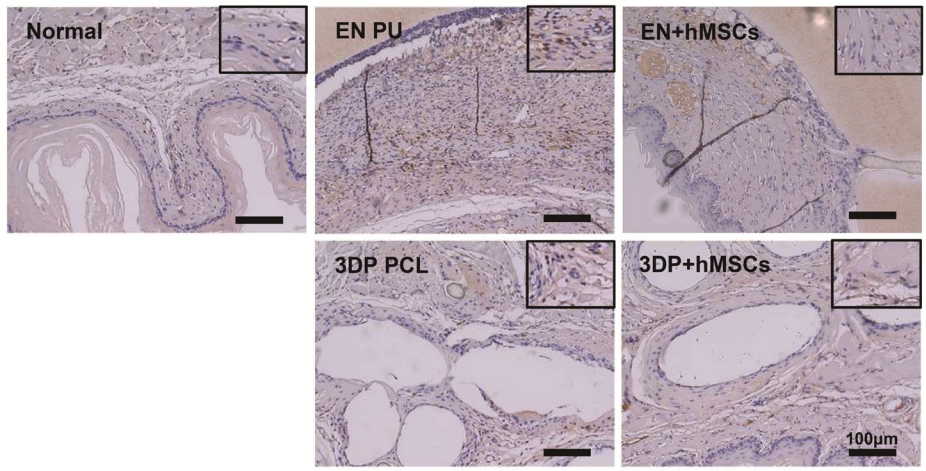

Figure 18. Immunohistochemical staining of macrophages expression at 4 weeks after implantation. Representative image showing the infiltration of macrophages by CD68 expression. (Brown dots, CD68-positive cells.

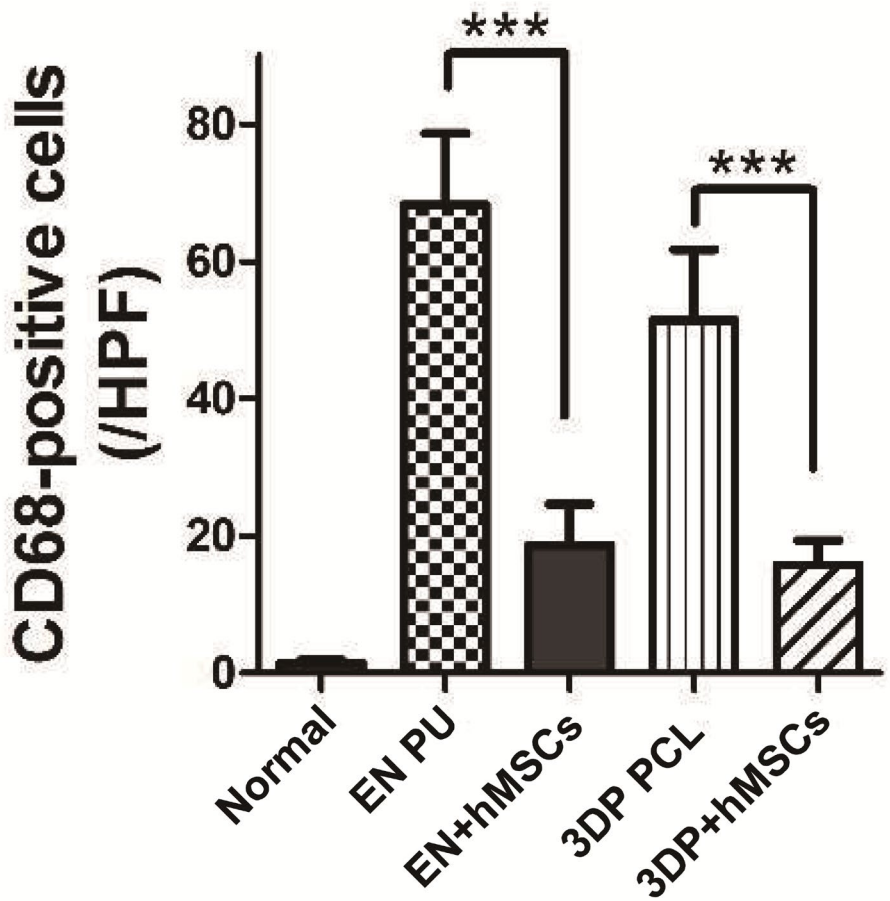

Figure 19. Statistical analysis of the number of CD68-positive macrophages per high-power field.

*. $p < 0.05$

**. $p < 0.01$

***. $p < 0.001$

국문초록

두 가지 유형의 조직 공학 스캐폴드를 사용한 이상적인 식도 재건에 대한 쥐 모델 실험 연구

박하나로

의학과 이비인후과학 전공

서울대학교 대학원

서론: 식도암, 식도 기형 등의 질환에 대한 치료 중 식도 결손이 일어날 수 있으며, 식도 결손에 대한 재건의 기존 방법들은 여러 합병증에 의하여 심하면 사망에 이르는 결과를 가져올 수 있다. 이에 조직 공학을 이용한 대안이 최근 각광받고 있다. 본 연구에서는 조직 공학을 이용하여 제작된 두 유형의 스캐폴드를 쥐 모델에 이식해 이들의 특성과 이식 결과에 대해 평가하였다.

재료 및 방법: 쥐 모델에 식도의 부분 결손을 재현한 후, 폴리카프로락톤으로 구성된 3D 프린팅 스캐폴드와 인간 지방 유래 중간엽 줄기세포로 처리한 폴리카프로락톤 3D 프린팅 스캐폴드, 폴리우레탄으로 구성된 전기 방사 나노섬유 스캐폴드와 인간 지방 유래

중간엽 줄기 세포로 처리한 전기 방사 나노섬유 스캐폴드를 각각 이식한 4개의 그룹으로 나누었다. 수술 후 1주 후와 4주 후에 각 그룹의 신체 상태, 체중, 혈액 검사 그리고 이식된 부위에 대하여 영상학적 검사와 조직 검사를 시행하여 평가하였다.

결과: 전기 방사 나노섬유 스캐폴드의 표면은 무작위 섬유 구조를 보여준 반면 3D 프린팅 스캐폴드는 여러 층을 이루는 구조를 구성하였다. 스캐폴드에 부착된 세포의 수는 전기 방사 나노섬유의 그룹이 3D 프린팅 그룹보다 많았다. 또한 생체 내 이식 결과, 모든 그룹의 결손은 누공 없이 재건되었으며, 점막하 고유층의 재생이 이식 후 4 개 그룹 모두에서 관찰되었다. 식도 근육은 인간 지방 유래 중간엽 줄기세포로 처리한 폴리카프로락톤 3D 프린팅 스캐폴드에서 전기 방사 나노섬유 스캐폴드에 비해 많이 관찰되었고, 재생된 상피의 두께는 3D 프린팅 그룹보다 전기 방사 나노섬유 그룹에서 유의하게 두꺼웠다. 신생혈관 형성은 인간 지방 유래 중간엽 줄기세포로 처리된 그룹들에서 현저하게 촉진되었고, 대식세포의 발현은 인간 지방 유래 중간엽 줄기세포로 처리된 그룹들에서 유의하게 적게 관찰되었다.

결론: 두 유형의 조직공학을 이용한 스캐폴드에서 모두 성공적인 이식 결과가 나타났다. 폴리 우레탄 전기 방사 나노섬유 스캐폴드에서 상피 재생이 많은 경향이 관찰되었고, 폴리카프로락톤 3D 프린팅 스캐폴드에서 식도 근육 재생이 많은 경향이 발견되었다.

주요어: 식도, 조직공학, 재생, 전기방사, 나노섬유, 3D 프린팅, 스캐폴드

학 번: 2017-21951